

## MORPHOLOGICAL, STRUCTURAL AND THERMAL PROPERTIES OF CHITOSAN/GRAPHENE OXIDE BIONANOCOMPOSITES

Aung Than Htwe<sup>1</sup>, Naing Min Tun<sup>1</sup>, Myo Min Soe<sup>1</sup>, Masao Gohdo<sup>2</sup>,  
Yoichi Yoshida<sup>3</sup>, Ni Ni Than<sup>4</sup>

### Abstract

Graphene oxide (GO) has been successfully synthesized from graphite powder using the Hummer's method. In this research, an ecofriendly bionanocomposite material has been fabricated from chitosan (CS)/graphene oxide (GO) by the casting method. The synthesized GO and CSGO were characterized by using FT IR, XRD, FESEM, TG-DTA and UV-Vis spectroscopy. Finally, the size and surface charge of synthesized nanoparticles were determined using the dynamic light scattering (DLS) and zeta potential analyzer, respectively. The results obtained from those different studies revealed that chitosan and graphene oxide could mix with each other homogeneously.

**Keywords:** chitosan, graphene oxide, Hummer's method, bionanocomposite

### Introduction

Nanocomposites are materials which consist of two components, with one of them having dimensions in nanometers ( $10^{-9}$  m) range (Bahal *et al.*, 2019). With the worsening of environmental problems, more and more attention has been attached to green chemistry. Chitosan (CS), a widely used polysaccharide, is the second largest renewable biopolymer after cellulose (Gong *et al.*, 2009). Solubility and poor mechanical properties of chitosan limit its widespread applications. Chitosan is insoluble in water but dissolves in aqueous solutions of organic acids like acetic, formic and citric acids. It can be used as a modifier due to the abundance of  $-NH_2$  and  $-OH$  functional groups which renders it ideal for a variety of chemical modifications (Pati *et al.*, 2015). The amine and two hydroxyl groups on each glucosamine monomer act as adsorption sites, especially the amine groups which are strongly reactive with metal ions. The cross-linking of chitosan is made between functional groups of chitosan and different kinds of cross-linking agents, such as glutaraldehyde, and epichlorohydrin (Liu *et al.*, 2012).

Graphene oxide is a hydrophilic carbon-based film enhancing the metal adsorption potential. The high surface area allows binding to metal oxides and the epoxy and carboxyl groups allows binding to biopolymers (Naicker *et al.*, 2019). Graphene oxide (GO), unlike graphene, has functional groups, e.g., carboxylic acid, epoxide, and hydroxyl groups, attached to a carbon sheet (Kosowska *et al.*, 2019). Graphene oxide (GO) may possess qualities for heavy metal adsorption that are superior to graphene. With all the promise and potential, relatively little is known about the safety of carbon-based nanomaterials, including nanotubes, graphene, and their derivatives (Dhawan *et al.*, 2019).

In the present study, chitosan (CS), glutaraldehyde cross-linked graphene oxide (GO) and chitosan/graphene oxide (CSGO) nanocomposites were prepared, and characterized. Finally the size and surface charge of synthesized nanoparticles were measured by dynamic light scattering and zeta potential analyzer, respectively.

---

<sup>1</sup> Lecturers, Department of Chemistry, University of Yangon, Myanmar

<sup>2</sup> Assistant Professor, The Institute of Scientific and Industrial Research, Osaka University, Japan

<sup>3</sup> Professor, The Institute of Scientific and Industrial Research, Osaka University, Japan

<sup>4</sup> Professor and Head, Department of Chemistry, University of Yangon, Myanmar

## Materials and Methods

Chitosan, with a deacetylation degree of about 90 %, was purchased from Boao Biological Tech. Co. Ltd in China. Graphite powder, analytical grade, was purchased from BDH. The other reagents, such as  $\text{CH}_3\text{COOH}$ ,  $\text{NaOH}$ , 98 %  $\text{H}_2\text{SO}_4$ ,  $\text{H}_2\text{O}_2$ ,  $\text{HCl}$ ,  $\text{KMnO}_4$ , glutaraldehyde and isopropyl alcohol, were supplied by Department of Chemistry, University of Yangon, Myanmar. All of the chemicals used in this study were of analytical grade. Solutions were diluted by using deionized water and distilled water.

### Preparation of Graphene Oxide (GO) Powder

The graphite powder was used to prepare GO according to the well-known Hummer's method with some modification. In brief, 3.0 g of graphite powder was placed in a beaker and then 98 % of sulphuric acid and 68 % of nitric acid were added in a 90:30 v/v ratio. During the reaction, the solution was in exothermic condition, so it must be stirred in the ice bath at 10 °C to maintain the temperature while the 9 g of  $\text{KMnO}_4$  was slowly added and stirred for 15 min after the temperature was controlled in the ice bath to 9 °C. 150 mL of distilled water was gradually added into the above solution under stirring with 300 rpm at 90 °C for 30 min to achieve neutral conditions. Then, 30 mL of hydrogen peroxide ( $\text{H}_2\text{O}_2$  30 %) was added to the solution, which was then stirred at 300 rpm for 1h. The resultant solution was centrifuged and washed with 600 mL hot distilled water to form a brown paste. 100 mL of 10 % hydrochloric acid was added and stirred for 30 min. Then, the precipitate was washed with 200 mL of distilled water five times at 7000 rpm for 30 min to get an acid-free mixture. The yellow-brown GO mixture was obtained. The obtained GO mixture was sonicated for 2 h and then centrifuged at 3000 rpm for 30 min. The GO dispersed mixture was purified using multiple washings with distilled water and ethanol until it reached neutrality (pH 7). After multiple washings, the solid GO was dried in oven at 80 °C to obtain dried GO.

### Preparation of Chitosan/Graphene Oxide Bionanocomposite

A 1 g of chitosan powder was dissolved in 100 mL of 1 % (v/v) acetic acid solution and was stirred continuously at room temperature to form 1 % chitosan (CS) solution. The 10 g of graphene oxide (GO) powder was dispersed into 100 mL of distilled water to form 10 % GO solution. The CSGO solutions were prepared with three different ratios of CS:GO, (95:5, 90:10, 85:15 v/v) by stirring the mixed polymer composite solution at 60 °C for 2 h. The mixture was sonicated at room temperature for 2 h to ensure a homogeneous dispersion of CSGO solution, after which 0.2 mL glutaraldehyde (50 % in  $\text{H}_2\text{O}$ ) was added dropwise with constant stirring. A black gel of CSGO solution was obtained. The mixed solution was cast on a glass plate and then dried in an oven at a temperature of 60 °C for 8 h. The dried CSGO films were removed from the glass plate, cut and powdered by using mortar and pestle. A series of chitosan/graphene oxide bionanocomposites coded as CSGO5 (CS/GO 95:5 %), CSGO10 (CS/GO 90:10 %), and CSGO15 (CS/GO 85:15 %) were prepared, respectively.

### Characterization

The surface morphology of bionanocomposite materials was studied using FESEM (Hitachi model SU 8000). FESEM images of samples were collected under an accelerating voltage of 5 kV. Fourier transform infrared spectrophotometer (Shimadzu, Japan) was used. The resolution was  $4\text{ cm}^{-1}$  with 64- time scanning, and the scanning was performed in the range of  $4000\text{--}500\text{ cm}^{-1}$ . The X-ray diffraction (XRD) measurements of CS, GO and CSGO bionanocomposites were recorded using Shimadzu 8000 X-ray diffractometer (Shimadzu, Japan) with a detector operating under a voltage of 40.0 kV and a current of 30.0 mA using  $\text{Cu K}\alpha$  radiation

( $\lambda = 0.15418$  nm). The recorded range of  $2\theta$  was  $5\text{--}40^\circ$ , and the scanning speed was  $6^\circ/\text{min}$ . The particle size distribution (PSD) of aggregates was measured using an optical microscope (Shimadzu, STZ-171 with Moticom U2.0MP, Japan), which captured the images. Dynamic light scattering (DLS) was used for the measurement of average particle size, and polydispersity index (PDI) on a high-performance particle Zetasizer Nano ZS (Model MALI034324, Malvern Instruments, UK).

## Results and Discussion

### Preparation and Characterization of CSGO Bionanocomposites

The CSGO bionanocomposites were successfully prepared by in situ mineralization, wherein the CSGO hydrogel was first prepared. CS is soluble in water at acidic pH, at which amine functional groups of the molecule undergo protonation.

### FT IR spectroscopy

FT IR experiments were carried out to investigate the interaction between GO and CS. As shown in Figure 1, in the spectrum of GO, the peaks at  $1039$ ,  $1321$ , and  $1620\text{ cm}^{-1}$  correspond to C–O–C stretching vibrations, C–OH stretching, and the C–C stretching mode of the  $\text{sp}^2$  carbon skeletal network, respectively, while peaks located at  $1716$  and  $3208\text{ cm}^{-1}$  correspond to C–O stretching vibrations of the –COOH groups and O–H stretching vibration, respectively. These functional groups make GO highly hydrophilic and render it dispersible (Maleki and Paydar, 2016). In the spectrum of CS, there are two characteristic absorption bands centered at  $1618$  and  $1581\text{ cm}^{-1}$ , which correspond to the C=O stretching vibration of –NHCO– and the N–H bending of –NH<sub>2</sub>, respectively. The GOCS spectra show peaks at  $3225$ ,  $3228$ ,  $3240\text{ cm}^{-1}$  (O–H distortion) and  $1618\text{ cm}^{-1}$ , as well as a superposition band assigned to the amine groups of CS and carboxyl groups of GO,  $1405\text{ cm}^{-1}$  and  $1149\text{ cm}^{-1}$ , indicating C–O bonds. Additionally, the characteristic signal of secondary amides (N–H bending) shifts from  $1538$  to  $1542\text{ cm}^{-1}$  (between the CS and GO-CS signals) (Figuerola *et al.*, 2020). Compared with pure CS and GO, both peaks at  $1581\text{ cm}^{-1}$  related to –NH bending vibration and at  $1718\text{ cm}^{-1}$  belonging to C=O stretching of the carboxyl group disappear in the spectra of CSGO bionanocomposites. Moreover, the band corresponding to the C=O characteristic stretching band of the amide group shifts to a lower wavenumber. These could be ascribed to the synergistic effect of hydrogen bonding between CS and the oxygenated groups in GO and electrostatic interaction between polycationic CS and the negative charge on the surface of GO (Han *et al.*, 2011).

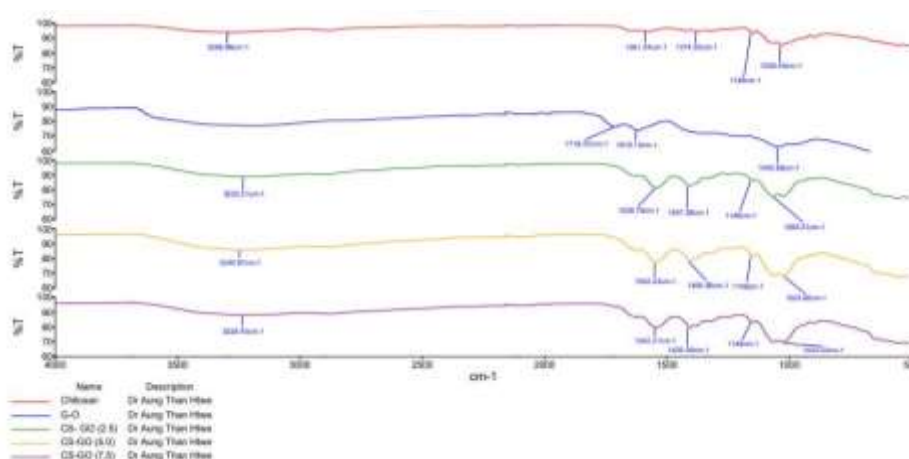
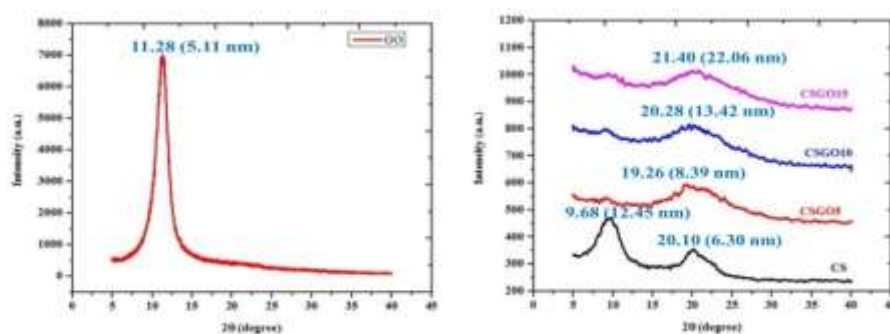


**Figure 1** FT IR spectra of GO, CS and CSGO bionanocomposites

## X-ray diffraction analysis

Figure 2 shows the XRD patterns of pure CS, GO and CSGO bionanocomposites. As seen in figure, the diffractive region of GO is observed at  $2\theta$  value of  $11.28^\circ$ . Pure chitosan showed a characteristic peak at around  $2\theta$  values  $9.68^\circ$  and sharp peak at  $20.10^\circ$ . The main diffractive region of all CSGO are found weak broad peak at  $2\theta$  value of  $11.85^\circ$  and weak broad peak at  $21.40^\circ$ . When incorporation of GO into CS chemical structure of the CS films changes due to overlap of biopolymer diffraction, it indicates that there was mainly physical interaction but scarcely chemical reaction between CS and GO (Han *et al.*, 2011).

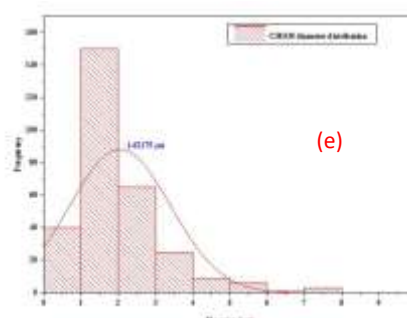
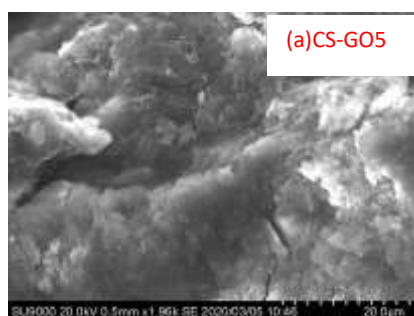
It is noticed that incorporation of CSGO only slightly increases the intensity of the characteristic peaks of CS. The CSGO bionanocomposite exhibited a combination of amorphous and crystalline peaks (Kumar and Koh, 2014). In this particular case, the electrostatic interaction and hydrogen bonding may contribute to a relatively ordered arrangement of the attached CS chains along the rigid template offered by GO (Yang *et al.*, 2010).



**Figure 2** XRD patterns of pure GO, CS and CSGO bionanocomposites

## FESEM-EDX Analysis

The morphology of the prepared CSGO5, CSGO10 and CSGO15 were investigated by field-emission-scanning electron micrographs (FESEM) technique. The surfaces of the CSGO5, CSGO10 and CSGO15 display a generally smooth morphology, as shown in Figures 3a–d, indicating that the chitosan films blending with graphene oxide are miscible. In addition, the surface of the composite films showed high homogeneity. The blending graphene oxide is wrapped in or covered by a chitosan layer. There is barely an isolated fully exfoliated graphene oxide sheet, which indicates a good adhesion between the chitosan and the graphene oxide (Figuroa *et al.*, 2020; Yang *et al.*, 2010).



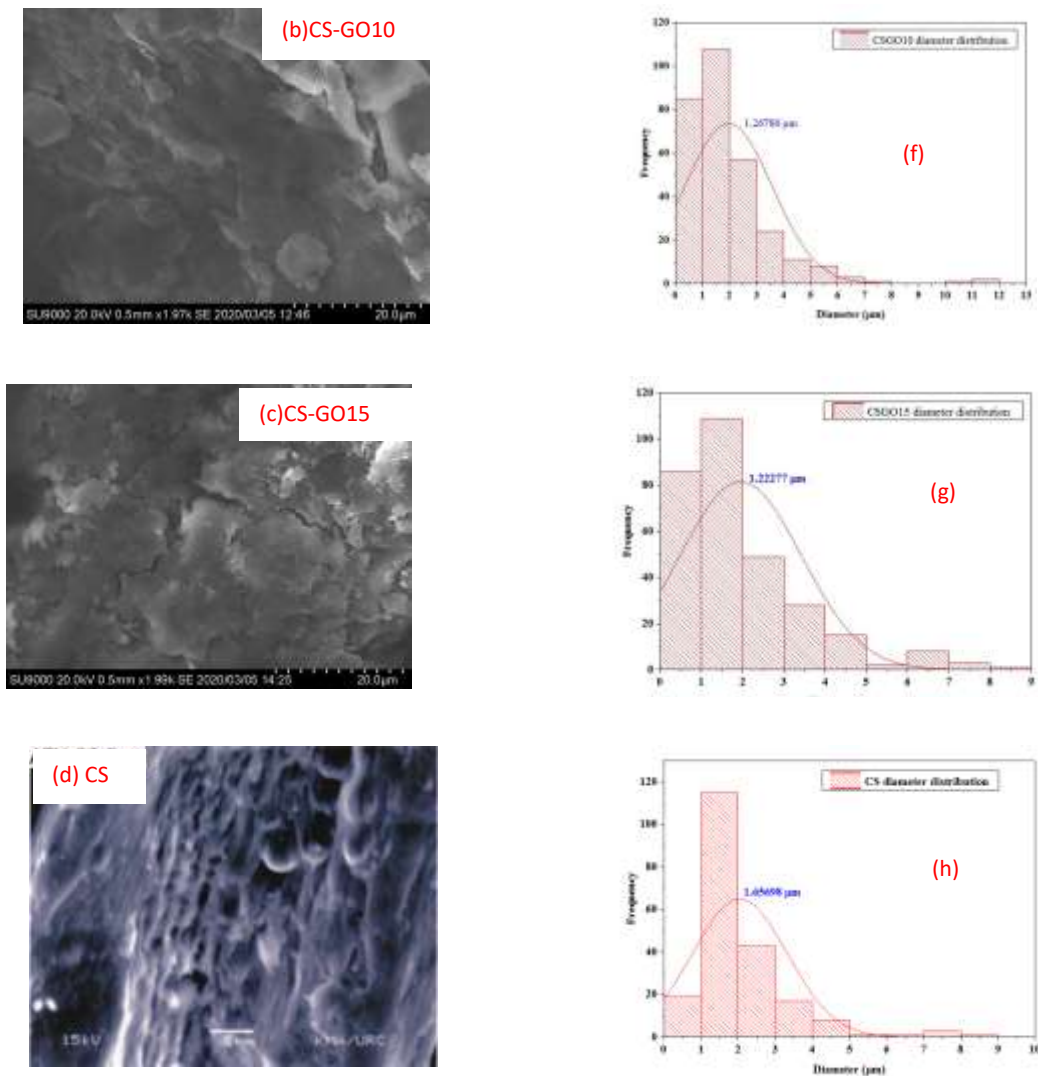


**Figure 3** FESEM images of CSGO bionanocomposites (a, b, c, d) and the corresponding statistical histograms (e, f, g, h)

Size diameter distributions (Figures 3 e-h) were evaluated by measuring at least 300 particles from FESEM micrographs. The results are obtained that the average diameters of the obtained bionanocomposites are 1.65  $\mu\text{m}$  for CS, 1.29  $\mu\text{m}$  for CSGO5, 1.26  $\mu\text{m}$  for CSGO10 and 1.22  $\mu\text{m}$  for CSGO15, respectively. The resulting nanocomposite have a significant size decrease (from 1.29  $\mu\text{m}$  for CSGO5 to 1.22  $\mu\text{m}$  for CSGO15), as can be seen from the size diameter distribution histograms. It indicates that the produced bionanocomposite possesses narrow size distribution.

To check the chemical composition of the material, an energy dispersive X-ray (EDX) spectroscopy analysis was also presented in Figure 4 and Table 1. The EDX spectra of CSGO bionanocomposite samples which confirm the presence of C, N, and O ions in the matrix. The EDX results are also consistent with the weight percentage of C, N, and O. From quantitative analysis it is evident that bionanocomposite samples contains approximately 62.84 % C, 1.24 % N and 35.92 % O by weight in CSGO5, 57.32 % C, 4.14 % N and 38.54 % O by weight in CSGO10, and 58.62 % C, 5.30 % N and 36.07 % O by weight in CSGO15, respectively. These results were found to be consistent with the XRD data.

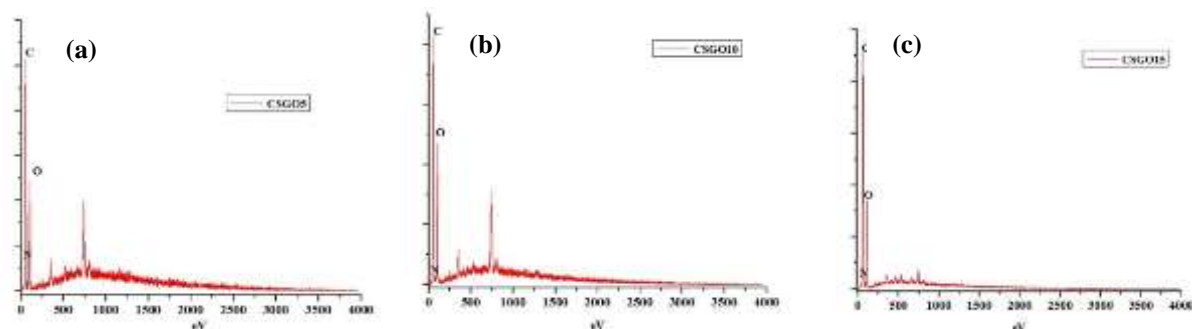


**Figure 4** EDX spectra of (a) CSGO5, (b) CSGO10, and (c) CSGO15

**Table 1** Compositional Analysis of the CSGO by EDX

Sample	Atomic % in bionanocomposites		
	C	N	O
CSGO5	62.84	1.24	35.92
CSGO10	57.32	4.14	38.54
CSGO15	58.62	5.30	36.07

### Thermogravimetric analysis

The thermal stability of the pure GO and three different ratios of CS/GO composite powder (CSGO5, CSGO10 and CSGO15) was studied by thermogravimetric analysis as shown in Figure 5(a) and (b). As seen in Figure 5(a) and (b), the thermal stability of GO was observed because of the weight loss of 75.28 % within the temperature range of 38 °C to 218 °C. This attributes to the thermal decomposition of unstable groups containing oxygen and evolution of CO<sub>2</sub> gas. The thermograms of all CSGO composites are shown in Figure 5(a) and (b), with weight loss in three stages. The first stage ranges in temperature from 37 °C to 155 °C, with weight loss of 22.15 % in CSGO5, 18.85 % in CSGO10 and 19.75 % in CSGO15. There is evaporation of water. The second stage, with temperature ranging from 155 °C to 426 °C, was observed to lose 38.77 % in CSGO5, 40.06 % in CSGO10, and 39.42 % in CSGO15 corresponding to the exothermic peaks at 313 °C, 307 °C, and 282 °C, respectively. This is due to a complex process including the degradation of the saccharide ring. In the third stage, the temperature ranges from 426 °C to 600 °C, and weight loss of 33.23 % in CSGO5, 32.99 % in CSGO10, and 36.61 % in CSGO15 corresponds to the broad exothermic peaks at 527 °C, 543 °C, and 502 °C. In this stage, weight loss is due to complete degradation of polymer. The results show that the maximum weight loss percent of GO is higher than that of CSGO bionanocomposites.

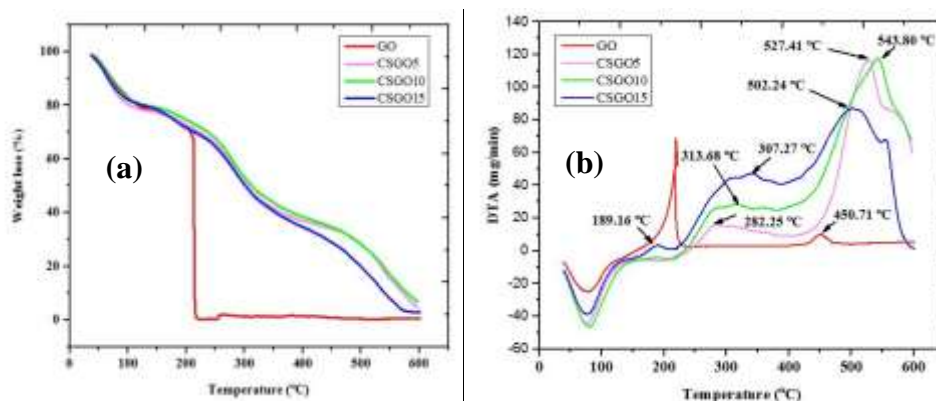


**Figure 5** (a)TG curves (b) DTA curves for GO and CSGO bionanocomposites

**UV-vis absorption spectra**

The UV-Vis spectrum (Figure 6) of pure GO shows two absorption peaks one at 229 nm and another at 335 nm (Wong *et al.*, 2015; Xu *et al.*, 2013). The CS peaks shows at 239 nm and 246 nm. The CSGO bionanocomposite shows 226 nm, 262 nm and 363 nm for CSGO5, 225 nm, 311 nm and 349 nm for CSGO10, and 227 nm and 325 nm for CSGO15. It was found that the intensity of CSGO bionanocomposite is lower than that of CS and GO. After attachment with CS, the peaks of GO have shown a bathochromic shift. This shift in absorption maxima might be attributed to the formation of particles in the nano scale. This also indicates the strong covalent interaction between GO and CS where the active ester group of GO might have reacted with the amine groups on CS, forming an amide bond between GO and CS (Suneetha, 2018).

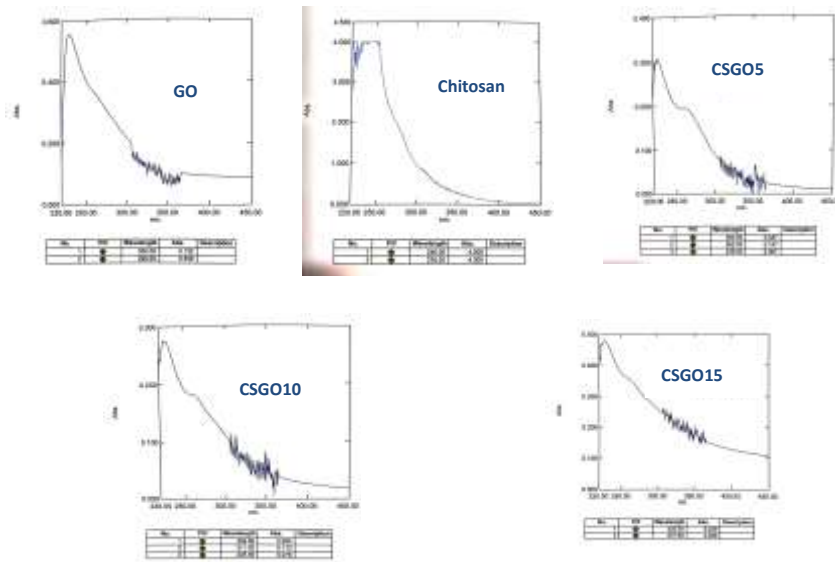


**Figure 6** UV-vis spectra of GO, CS and CSGO bionanocomposites

**Optical microscopy**

Size data were obtained by image processing and analysis obtained from samples studied by optical microscopy. Figure 7 shows the optical micrographs captured by the camera for GO and CSGO samples. It was found that the samples of CSGO showed the lowest particle sizes prior to particle size measurement by optical microscopy (52.29  $\mu\text{m}$  for CSGO5, 31.29  $\mu\text{m}$  for CSGO10 and 28.39  $\mu\text{m}$  for CSGO15, respectively). Among them, CSGO15 had a higher quantity of aggregates with fewer fine particles around the large aggregates. In this case, pure CSGO bionanocomposites have a higher quantity of aggregates with fewer fine particles around the large aggregates. Therefore, the image capture must be very fast. Therefore, the results obtained from image analysis captured by optical microscopy were non-invasive. These results can thereby determine more realistic particle sizes of the aggregates (Quilaqueo *et al.*, 2019).

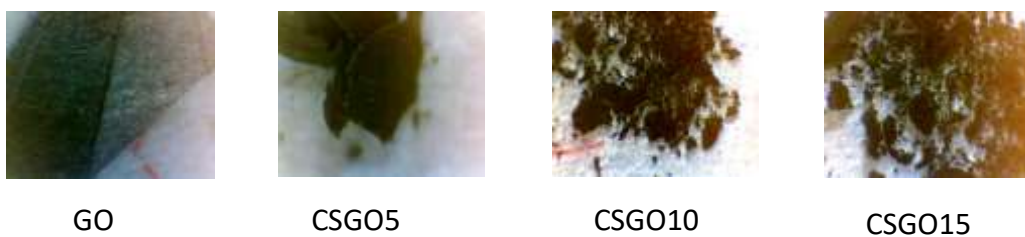


**Figure 7** Optical micrographs of pure GO and CSGO bionanocomposites

## Particle Size Study of GO and CSGO by Dynamic Light Scattering

The DLS experiment was conducted at a constant temperature of 25 °C. Figure 8 shows the size distribution graphs for the GO and CSGO bionanocomposites obtained by DLS method according to size distribution data analysis. The DLS results showed the presence of CSGO nanoparticles with a size of approximately 594.6 nm for CSGO5, 686.5 nm for CSGO10, 1383.0 nm for CSGO15 and the presence of larger particles, which corresponded to the GO carrier (498.5 nm). It was found that the increasing the GO content of 5 %, 10 % and 15 %, the lower the average diameter. Therefore, it can be observed that the average diameter of all of the prepared CSGO bionanocomposite are higher than that of pure GO. These reveal that ranges of distribution of the resultant CSGO bionanocomposites were wider than that of GO. This also confirms the binding of CS and GO bionanocomposites that leads to larger-size (Zeinali *et al.*, 2016).

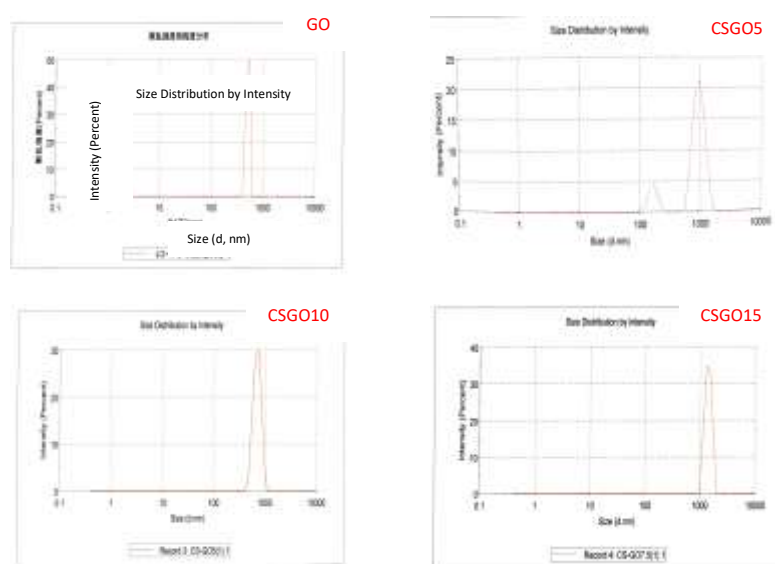


**Figure 8** Particle size distribution of GO and CSGO bionanocomposites

## Zeta Potential Measurement

Although  $\zeta$ -potential plays a key role in colloidal stability, it does not show the true particulate state in various environments. To estimate the aggregation behaviour of GO and CSGO samples under aging conditions, visual evidence of settling was used. All the GO samples show excellent colloidal dispersity and stability in deionized water after 24 h at 37 °C. At higher pH, the oxygenated functional groups such as hydroxyl and carboxyl of GO and CSGO could be easily deprotonated, leading to a favourable electrostatic attraction with the cationic CS. In order to further support our hypothesis, zeta potential measurements were conducted for GO and CSGO nanocomposites at neutral solutions, and the results are presented in Figure 9.

It was found that the zeta potential value of pure GO is about  $-25$  mV because of  $-\text{COO}^-$  groups on the GO (Karimzadeh *et al.*, 2019). All the CSGO bionanocomposites showed  $+37.7$  mV for CSGO5,  $+34.6$  mV for CSGO10 and  $+39.6$  mV for CSGO15, respectively (Table 2). So the positive zeta potentials for CSGO were consistent with the presence of protonated amine groups of CS. It is well known that higher absolute value of zeta potential means higher stable state of colloidal systems, and potential values higher than  $+30$  mV or lower than  $-30$  mV permit a basically stable suspension (Sun *et al.*, 2016).

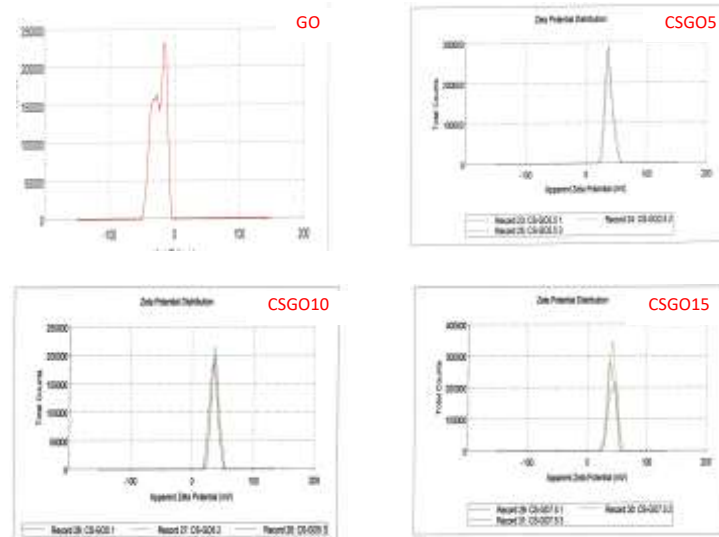


**Figure 9** Zeta potential measurement of GO and CSGO bionanocomposites

**Table 2** The Zeta Potential and Calculated Average Diameter of the GO and CSGO

Sample	Zeta potential (mV)	Average diameter calculated by laser particle size (nm)
GO	- 25.0	498.5
CSGO5	+ 37.7	594.6
CSGO10	+ 34.6	686.5
CSGO15	+ 39.6	1383.0

### Conclusion

The bionanocomposites of chitosan/graphene oxide GO were prepared successfully by solvent casting method. It is observed that graphene oxide is dispersed on a molecular scale in the chitosan matrix and some interactions occur between chitosan and graphene. In CSGO bionanocomposites FT IR showed the existence of oxygen-containing functional groups of GO, amino groups of CS, and amide I groups forming from reaction between GO and CS. The XRD patterns implied amorphous state of CSGO. FESEM images confirmed the linking and grafting of CSGO. TG-DTA measurements indicated homogeneous dispersion of GO within the CS polymer matrix. The synthesized bionanocomposite was found to have greater thermal stability. Presence of both the components of the bionanocomposite was confirmed by UV-Vis and FT IR spectral studies. These studies also indicate the strong interaction between GO and CS in the bionanocomposites. The nanoparticles size and surface charge were measured by dynamic light scattering and zeta potential analyzer. DLS measurement was formed that the increasing the GO content, the larger will be the average diameter, All the results demonstrated that graphene oxide was well-dispersed in the chitosan matrix, and there were the strong H-bondings between hydroxy groups of the chitosan and hydroxy groups of the graphene oxide. The main contribution of the present research is that the synthesis of chitosan- graphene oxide bionanocomposite may be used for the control of wastewater pollution.

## Acknowledgements

The authors would like to thank the Department of Higher Education, Ministry of Education and University of Yangon for some support to do this research. This research was supported by the KAPLAT program (JSPS Core-to-Core) Japan and Osaka University for intensive 2020. We would like to acknowledge KAPLAT Program Coordinator Professor Dr Hideaki OHGAKI, Institute of Advanced Energy, Kyoto University. Finally, we are also thankful to Nanotechnology Open Facility, Osaka University, for providing zetasizer, XRD, and FESEM facilities.

## References

- Bahal, M., N. Kaur, N. Sharotri, and D. Sud. (2019). "Investigations on Amphoteric Chitosan/TiO<sub>2</sub> Bionanocomposites for Application in Visible Light Induced Photocatalytic Degradation". *Advances in Polymer Technology*, vol. 2019, pp. 1-9
- Dhawan, A. K., J. W. Seyler, and B. C. Bohrer. (2019). "Preparation of a Core-Double Shell Chitosan Graphene Oxide Composite and Investigation of Pb(II) Absorption". *Heliyon*, vol. 5(e01177), pp. 1-14
- Figueroa, T., C. Aguayo, and K. Fernandez. (2020). "Design and Characterization of Chitosan-Graphene Oxide Nanocomposites for the Delivery of Proanthocyanidins". *International Journal of Nanomedicine*, vol. 15, pp. 1229-1238
- Gong, Y., Y. Yu, H. Kang, X. Chem, H. Liu, Y. Zhang, Y. Sun, and H. Song. (2009). "Synthesis and Characterization of Graphene Oxide/Chitosan Composite Aerogels with High Mechanical Performance". *Polymers*, vol. 11 (777), pp. 1-12
- Han, D., L. Yan, W. Chen, and W. Li. (2011). "Preparation of Chitosan/Graphene Oxide Composite Film with Enhanced Mechanical Strength in the Wet State". *Carbohydrate Polymers*, vol. 83, pp. 653-658
- Karimzadeh, Z., S. Javanbakht, and H. Namazi. (2019). "Carboxymethyl Cellulose/MOF-5/Graphene Oxide Bio Nano Composite as Antibacterial Drug Nanocarrier Agent". *BioImpacts*, vol. 9 (1), pp. 5-13
- Kosowska, K., P. D. Pyzik, M. K. Borkowicz, and J. Chlopek. (2019). "Synthesis and Characterization of Chitosan/Reduced Graphene Oxide Hybride Composites". *Materials*, vol. 12 (2077), pp. 1-13
- Kumar, S., and J. Koh. (2014). "Physicochemical and Optical Properties of Chitosan Based Graphene Oxide Bionanocomposite". *International Journal of Biological Macromolecules*, vol. 70, pp. 559-564
- Liu, L., C. Li, C. Bao, Q. Jia, P. Xiao, X. Liu, and Q. Zhang. (2012). "Preparation and Characterization of Chitosan/Graphene Oxide Composites for the Adsorption of Au(III) and Pd(II)". *Talanta*, vol. 93, pp. 350-357
- Maleki, A., and R. Paydar. (2016). "Bionanostructure- Catalyzed One-Pot Three-Component Synthesis of 3,4-Dihydropyrimidin-2(1H)-One Derivatives Under Solvent-Free Conditions". *React. Funct. Polym.*, vol. 109, pp. 120-124
- Naicker, C., N. Nombona, and W. E. Zyl. (2020). "Fabrication of Novel Magnetic Chitosan/Graphene Oxide/Metal Oxide Nanocomposite Beads for Cr(VI) Adsorption". *Chemical Papers*, vol. 74, pp. 529-542
- Pati, M. K., P. Pattojoshi, and G. S. Roy. (2015). "Fabrication and Characterization of Graphene Based Nanocomposite for Electrical Properties". *Advances in Materials Physics and Chemistry*, vol. 5, pp. 22-30
- Quilaqueo, M., M. G. Krumm, R. R. Figueroa, E. Troncoso, and H. Estay. (2019). "Determination of Size Distribution of Precipitation Aggregates Using Non-Invasive Microscopy and Semiautomated Image Processing and Analysis". *Minerals*, vol. 9 (724), pp. 1-14
- Sun, D., S. Kang, C. Liu, Q. Lu, L. Cui, L., and B. Hu. (2016). "Effect of Zeta Potential and Particle Size on the Stability of SiO<sub>2</sub> Nanospheres as Carrier for Ultrasound Imaging Contrast Agents". *Int. J. Electrochem. Sci.*, vol. 11, pp. 8520 – 8529
- Suneetha, R. B. (2018). "Spectral, Thermal and Morphological Characterization of Biodegradable Graphene Oxide-Chitosan Nanocomposites". *J. Nanosci. Tech.*, vol. 4 (2), pp. 342-344
- Wong, C. P. P., C. W. Lai, K. M. Lee, and S. B. A. Hamid. (2015). "Advanced Chemical Reduction of Reduced Graphene Oxide and Its Photocatalytic Activity in Degrading Reactive Black 5". *Sci. Tech. Adv. Mater.*, vol. 8, pp. 7118-7128
- Xu, S., L. Yong, and P. Wu. (2013). "One-pot, Green, Rapid Synthesis of Flowerlike Gold Nanoparticles/ Reduced Graphene Oxide Composite with Regenerated Silk Fibroin As Efficient Oxygen Reduction Electrocatalysts". *ACS Applied Materials & Interfaces*, vol. 5, pp. 654-662
- Yang, X., Y., L. Li, S. Shang, and X. Tao. (2010). "Well-Dispersed Chitosan/Graphene Oxide Nanocomposites". *ACS Applied Materials & Interfaces*, vol. 2 (6), pp. 1707-1713
- Zeinali, S., S. Nasirimoghaddam, and S. Sabbaghi. (2016). "Investigation of the Synthesis Chitosan Coated Iron Oxide Nanoparticles under Different Experimental Conditions". *Int. J. Nanosci. Nanotechnol.*, vol. 12 (3), pp. 183-190